Simulations of photoconductivity and lifetime for steady state and nonsteady state measurements

N. Schüler,[1,a)] T. Hahn,[2] S. Schmerler,[2] S. Hahn,[1] K. Dornich,[1] and J. R. Niklas[1]
[1]*Freiberg Instruments GmbH, Am St. Niclas Schacht 13, 09599 Freiberg, Germany*
[2]*TU Bergakademie Freiberg, Leipziger Straße 23, 09596 Freiberg, Germany*

(Received 4 October 2009; accepted 30 January 2010; published online 16 March 2010)

Contact less measurements of the minority carrier "lifetime" and the photoconductivity are widely used to characterize the material quality and to investigate defects in a sample. In order to interpret these measurements correctly and to guarantee comparability between different methods, numerical simulation tools were developed. These simulations allow to account even for very complex defect models, thus, e.g., enabling the simulation of trapping effects. Contrary to the Shockley–Read–Hall model or the widely used simulation tool PC1D nearly no assumptions are made. Furthermore, nonsteady state solutions can be obtained. The simulation approach is explained in detail, along with simulations of the trapping effect on the measured lifetime for different injections, trap parameters, and measuring methods, demonstrating the capabilities of the here presented simulation tool. Temperature and injection dependent lifetime measurements were performed and it is shown how important sample parameters can be extracted using the simulation tool. Additionally an approach is presented to simulate lifetimes for thick samples, where a nonuniform carrier profile has to be taken into account. This enables a comparison of nonsteady state to steady-state lifetime measurement techniques even for thick samples such as ingots. © *2010 American Institute of Physics*. [doi:10.1063/1.3331628]

I. INTRODUCTION

Lifetime measurements are becoming more and more important for the investigation of even very small concentrations of defects in semiconductors and as a fast method to characterize the material quality. Most contact less methods like quasisteady state photoconductivity (QSSPC), (microwave detected photoconductance decay) (μPCD), or (microwave detected photoconductivity (MDP) measure the minority carrier "lifetime" via time resolved photoconductivity measurements during and after the excitation of the sample with a flash light or laser beam. Additionally, the steady state photoconductivity contains a lot of information itself about the mobility and the diffusion length of the carriers.

Unfortunately, the measurement results of different methods can deviate strongly, especially between steady-state and nonsteady state methods. For thick as-grown samples these differences can be even more pronounced because of the different nonuniform carrier profiles, which develop in the sample.

Furthermore most of the contact less and destruction free methods such as QSSPC, μPCD, or MDP suffer from trapping effects at low injections. It became obvious, that the Shockley–Read–Hall (SRH) model[1] or other rather simple trapping models are of only limited value for the interpretation of the measurement results.

The Shockley–Read–Hall model is limited by the assumption that the excess carrier concentration generated during the measurement obeys $\Delta n = \Delta p$, which is invalid if trapping occurs. The often used analytical model of Hornbeck and Haynes[2] assumes, that an interaction of a trap is only possible with one band (conduction or valence band) and that the corresponding defect level is unoccupied at equilibrium and fully occupied under illumination. Furthermore a constant lifetime τ_{LLI} is used in this model. However, for very high trap densities and a recombination center with very asymmetric capture cross sections, this can be inadequate.

McIntosh *et al.*[3] presented a procedure to overcome most of these restrictions. Their model, however, is only valid for steady state measurements, a constant mobility, and it does not account for temperature dependent capture cross sections.

Contrary to that, the here presented simulation tool via a generalized rate equation system works nearly without any assumptions. With this tool and an additional approach for nonuniform carrier profiles all problems mentioned above can be solved. Experimental results confirming the simulations for some exemplary cases are presented as well.

II. SIMULATION

A. The generalized rate equation system

The numerical tool is based on a generalized rate equation system. The rate equations are used to describe the time dependent change in the carrier occupation of the bands ($\dot{n}, \dot{p}$) and defects ($\dot{n}_{Tj}$). All possible transitions between the defect levels in the forbidden gap and the bands of a semiconductor are described by transition rates.

This simulation tool is based on the work of Brasil and Motisuke[4] and Yoshie and Kamihara[5] which used a simple rate equation system to explain the carrier dynamics in conventional photoinduced carrier transient spectroscopy mea-

a)Electronic mail: schueler@freiberginstruments.com.

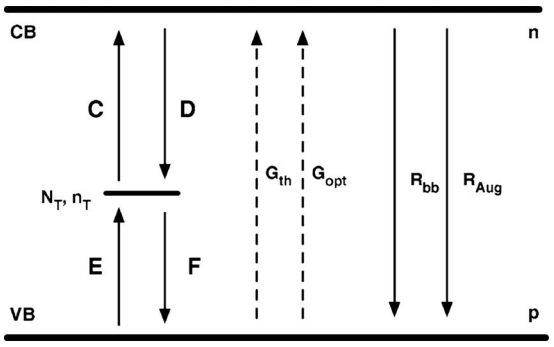

FIG. 1. Energy scheme including all transitions, that are considered in the simulations (Ref. 7).

surements. This rate equation system implies, however, several restrictions like the assumption of a constant lifetime.

Schmerler and Hahn[6,7] developed a rate equation system, in which the only approximation is, that no direct interactions between defect levels are included.

$$\dot{n} = G_{\mathrm{BB}}^{o} + G_{\mathrm{BB}}^{th} + \sum_{j} (C_j - D_j) - U_{\mathrm{BB}} - U_{\mathrm{Aug}}, \tag{1}$$

$$\dot{p} = G_{\mathrm{BB}}^{o} + G_{\mathrm{BB}}^{th} + \sum_{j} (F_j - E_j) - U_{\mathrm{BB}} - U_{\mathrm{Aug}}, \tag{2}$$

$$\dot{n}_{Tj} = D_j + E_j - C_j - F_j. \tag{3}$$

Figure 1 displays all transition rates, that are included in the rate equation system. The optical and thermal generation rates $(G_{\mathrm{BB}}^{o}, G_{\mathrm{BB}}^{th})$, the band to band and Auger recombination rates $(U_{\mathrm{BB}}, U_{\mathrm{Aug}})$ and the carrier capture (D_j, E_j) and emission rates for all defects (C_j, F_j) are included. The transition rates are described without any approximations, e.g., the emission rate of an electron is described by

$$C = n_T(t)\sigma_n v_{th} \exp\left(-\frac{E_{\mathrm{C}} - E_T}{k_B T}\right)[N_C - n(t)], \tag{4}$$

[fermi statistic is used for shallow defects instead of Eq. (4)]. Other transition rates are expressed in a similar way.

As mentioned before, an arbitrary number of defects can be included into the simulation. For every defect the following defect parameters have to be included

- Defect concentration N_{Tj}.
- Activation energy E_{Tj}.
- Capture cross sections for electrons and holes, σ_n and σ_p.
- Occupation type D^- or A^+ (representing donor or acceptor like behavior of the defect).

A trapping or a recombination center can thus be introduced by adjusting the capture cross sections. A trapping center interacts mainly with only one band, which means one of the two capture cross sections is nearly zero, where as a recombination center interacts with both bands. To include a certain doping concentration into the simulations, the corresponding number of acceptors and donors has to be inserted.

The rate equation system is solved numerically with appropriate ordinary differential equation solvers.[8,9] First of all the thermodynamic equilibrium occupations of the bands and every defect level are computed with $G_{\mathrm{opt}}=0$. The results of this calculation are used as initial values for the determination of the changes in the occupation of the defect levels during the light pulse $(G_{\mathrm{opt}}>0)$. For this simulation an average optical generation rate is used so that this simulation tool is only valid for the measurements of thin samples developing a uniform carrier profile. Of course, also the effects of a slow decay of the light intensity as in QSSPC measurements or a turned-off laser beam can now be accounted for using the last occupation of the levels under illumination as initial values for following calculations.

Based on the simulated time dependent carrier concentrations, the photoconductivity can be calculated using the mobility model of Dorkel and Leturcq.[10] The minority carrier lifetime finally can be extracted from the simulated transient decay of the photoconductivity after G_{opt} is set to zero or can be determined from the photoconductivity value, if a quasi-steady state approach is used. Consequently, the technique which is used to evaluate the lifetime values from the simulated data is strictly based on the used measurement technique and thus is similar to the lifetime evaluation technique which is experimentally applied. Therefore, a very good agreement between simulated values and measurement results is guaranteed.

B. Nonuniform carrier profiles

If thick samples (W > 500 μm) are considered using the above techniques the laser or flash light excitation usually results in an inhomogeneous carrier profile and hence the carrier density depends strongly on the sample depth. The simulation of such a depth dependent carrier profile is achieved using a partial differential equation system, which is directly derived from the carrier transport equations.[11]

$$\frac{\partial}{\partial t}n(x,t) = \frac{\partial}{\partial x}\left[-\mu_n n(x,t)\frac{\partial}{\partial x}\Psi(x,t) + D_n\frac{\partial}{\partial x}n(x,t)\right] + G^{o}(x,t) - U(x,t), \tag{5}$$

$$\frac{\partial}{\partial t}p(x,t) = \frac{\partial}{\partial x}\left[\mu_p p(x,t)\frac{\partial}{\partial x}\Psi(x,t) + D_p\frac{\partial}{\partial x}p(x,t)\right] + G^{o}(x,t) - U(x,t), \tag{6}$$

$$\frac{\partial^2}{\partial x^2}\Psi(x,t) = -\frac{q}{\varepsilon_0\varepsilon_r}[-n(x,t) + p(x,t) \pm N_{\mathrm{dot}}], \tag{7}$$

where $\Psi(x,t)$ is the electrostatic potential, $\mu_{n,p}$ is the electron and hole mobility, $D_{n,p}$ the diffusion constant for electrons and holes, $G^{o}(x,t)$ is the generation rate, $U(x,t)$ the recombination rate, and N_{dot} is the doping concentration.

This equation system includes carrier diffusion, drift currents, and generation and recombination processes. The recombination term combines band to band recombination, Auger recombination and SRH recombination and is defined by the resulting injection dependent bulk lifetime, which can be derived from the rate equation system explained above.

$$U(x,t) = \frac{\Delta n(x,t)}{\tau_{\text{bulk}}[\Delta n(x,t)]}. \tag{8}$$

The partial differential equation system can be solved by utilizing the method of lines.[12]

The initial conditions are the equilibrium carrier concentrations n_0 and p_0, and the boundary conditions are defined by the surface recombination velocity. Hence, the simulation of passivated or as-grown surfaces is possible.

Based on the simulated carrier profiles a weighted average carrier density for every time spot can be evaluated as follows:[13]

$$\Delta n_{\text{avg}} = \frac{\int_0^W \Delta n(x) w(x) dx}{\int_0^W w(x) dx}, \tag{9}$$

with $w(x) = e^{-(x/\delta)}$, where δ is the skin depth of the penetrating microwave applied during the measurement. From the transient decay of this average carrier density the effective lifetime can be extracted, which should closely agree to the measured lifetimes.

III. EXPERIMENTAL METHOD

Several SiN_x passivated, *p*-type multicrystalline (mc)-Si wafers with a doping concentration of approximately 10^{16} cm^{-3} and a thickness of 180 μm were measured, using the MDP method. All wafers were passivated with SiN_x, so that the surface recombination can be neglected. The samples were illuminated with light and the time-dependent photoconductivity was measured. The "apparent lifetime" was extracted from the decay of the photoconductivity after the light has been switched-off. The MDP method allows to adjust the duration of the light pulse from 3 μs to several milliseconds, thus allowing to measure in a steady-state or nonsteady-state regime.

For temperature dependent measurements the wafers were cut in 1 cm^2 pieces and inserted into a cryostat, which was cooled down with liquid nitrogen to 100 K and subsequently heated up to 500 K.

In addition some as-grown mc-Si ingots were mapped by MDP and μPCD to investigate the different results at different measurement conditions at thick samples.

IV. RESULTS

A. Trapping center

As mentioned above, the application of the rate equation system makes it possible to investigate the influence of traps on the apparent lifetime. An arbitrary number of traps and recombination centers can be included into the simulations and the occupation for every defect level is computed.

Figure 2 shows the influence of different trapping parameters on the apparent lifetime. The defect model of McIntosh[3] was used to allow a direct comparison of the results. Apparent lifetime τ_{app} is a value one simply obtains by evaluating the observed or simulated conductivity decay as if it would reflect the carrier lifetime. This is attributed to as lifetime in the following. As seen below the errors might be dramatic.

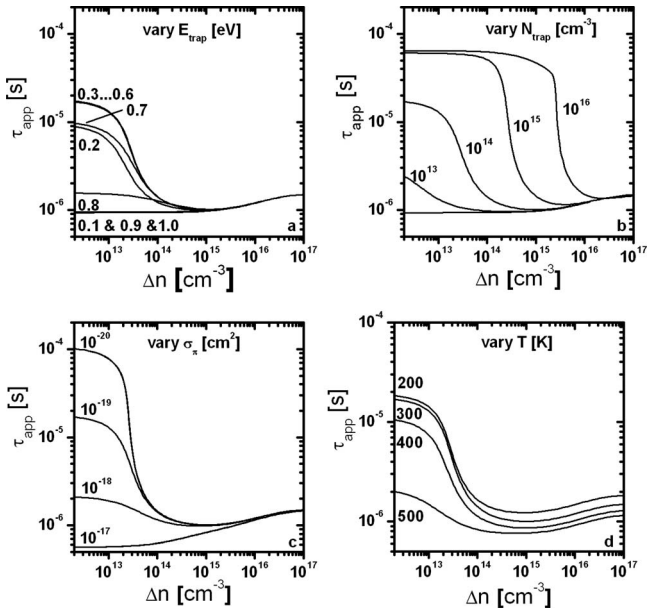

FIG. 2. τ_{app} vs injection Δn for *p*-type silicon with $N_{\text{dot}} = 10^{16}$ cm^{-3} at 300 K. The parameters of the recombination center are $N_{\text{rc}} = 10^{14}$ cm^{-3}, $\sigma_n = \sigma_p = 10^{-15}$ cm^2, and $E_{\text{rc}} - E_i = 0$ eV and those of the trap are $N_{\text{trap}} = 10^{14}$ cm^{-3}, $\sigma_n = 10^{-15}$ cm^2, $\sigma_p = 10^{-19}$ cm^2, and $E_{\text{trap}} = 0.3$ eV. The trap parameters are consecutively changed to show the impact of different trap parameters on the apparent lifetime. Thus the apparent lifetime is depicted for (a) different trap activation energies, (b) a varying trap density, (c) a varying capture cross section for holes, and (d) different temperatures are displayed.

As it is shown in Figs. 2(a)–2(c) the results previously reported by McIntosh are reproduced by the application of the rate equation system, indicating that the simulation tool works correctly. The main difference to the simulations of McIntosh are, that temperature dependent capture cross sections are used, which becomes obvious in Fig. 2(d), where a temperature dependent lifetime is observed. Since temperature dependent lifetime measurements are used for the investigation of defects,[14] it is very important to simulate these dependencies correctly.

The major challenge is to convey the experience gained by the here presented simulations to measurements, thus using it to extract parameters of the recombination center and/or the trap from real measurements. Figure 3 shows temperature dependent lifetime measurements performed at a *p*-type mc-silicon wafer, which were done from 100 to 500 K. Three different optical generation rates were used, showing that the trapping effect on the measured lifetime decreases with an increasing generation rate. Since there are a lot of free parameters in the simulation model some reasonable assumptions has to be made, in order to fit these measured lifetime curves. One assumption is, that there is only one dominant recombination and one trap center, with the latter only interacting with the conduction band. By variation in the residual free parameters the measured lifetime curves can be fitted. Since the characteristic rise of the lifetime with temperature due to the recombination center is only observable at high temperatures and generation rates, a large error can occur for the determination of the accordant energy level. It was determined to be $E_C - (0.15 \pm 0.1)$eV with a symmetry factor of $k = 0.35 \pm 0.20$ and a density of

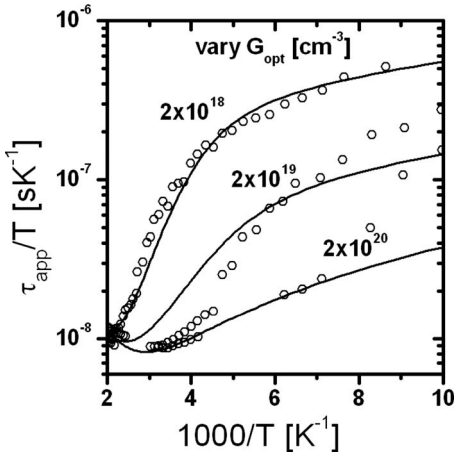

FIG. 3. Arrhenius plot of the measured apparent lifetime (circles) for different optical generation rates [cm^{-3} s^{-1}]; fitted lifetime curves (lines) obtained by generalized rate equations with a recombination center defined by $N_{rc}=2\times10^{13}$ cm^{-3}, k=0.35±0.20, and $E_{rc}=E_C-(0.15\pm0.1)$eV and a trapping center defined by $N_{trap}=4\times10^{14}$ cm^{-3}, $\sigma_n=5\times10^{-14}$ cm^2, $\sigma_p=0$ cm^2, and $E_{trap}=E_C-0.2$ eV.

$N_{rc}=2\times10^{13}$ cm^{-3}. The symmetry factor is defined as σ_n/σ_p and is often used to describe recombination centers since the determination of exact capture cross sections is very difficult. One known recombination center fulfilling the conditions, that were measured is FeB.[15] The parameters of the trapping center were determined to be $N_{trap}=4\times10^{14}$ cm^{-3}, $\sigma_n=5\times10^{-14}$ cm^2, $\sigma_p=0$ cm^2, and $E_{trap}=E_C-0.2$ eV by fitting the measured curves.

Figure 4 displays injection dependent measurements of three *p*-type mc-silicon wafers of different heights of an ingot. The doping concentration of these samples is approximately 10^{16} cm^{-3} and varies only little between these three samples. Similar to the results in Fig. 3 one recombination and one trapping center were assumed. Unfortunately, the actual energy level of the recombination center cannot be determined because of the strong trapping influence at low injections. That is why a midgap recombination center was

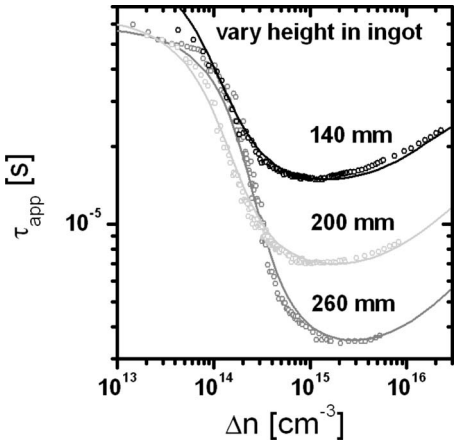

FIG. 4. Measured apparent lifetime vs injection (circles) for wafers of different height of an mc-Si ingot; fitted lifetime curves (lines) obtained by generalized rate equations with a recombination center defined by $N_{rc,140\ mm}=2.5\times10^{12}$ cm^{-3}, $N_{rc,200\ mm}=6.0\times10^{12}$ cm^{-3}, $N_{rc,260\ mm}=1.3\times10^{13}$ cm^{-3}, k=5, and $E_{rc}=0.56$ eV and a trapping center defined by $N_{trap,140\ mm}=3\times10^{14}$ cm^{-3}, $N_{trap,200\ mm}=4\times10^{14}$ cm^{-3}, $N_{trap,260\ mm}=8\times10^{13}$ cm^{-3}, $\sigma_n=5\times10^{-14}$ cm^2, $\sigma_p=0$ cm^2, and $E_{trap}=E_C-0.35$ eV.

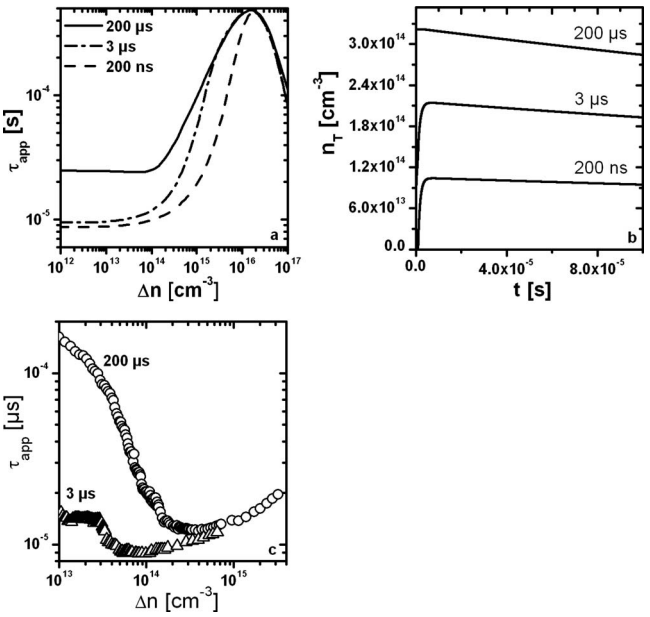

FIG. 5. τ_{app} vs injection for three different lengths of the exciting laser pulse (a) and captured electron concentration vs time after the light has been switched-off ($t=0$ µs) (Ref. 16), (b) the following parameters were used for the simulation: recombination center Fe_i (Ref. 15) defined by $N_{rc}=10^{12}$ cm^{-3} $\sigma_n=3.6\times10^{-15}$ cm^2, $\sigma_p=6.8\times10^{17}$ cm^2, and $E_{rc}=E_V+0.394$ eV and a trapping center defined by $N_{trap}=1\times10^{14}$ cm^{-3}, $\sigma_n=1\times10^{-16}$ cm^2, $\sigma_p=0$ cm^2, and $E_{trap}=E_C-0.35$ eV; measured lifetime curves with 3 and 200 µs pulse length (Ref. 16) (c).

assumed. However, all three lifetime curves were fitted with the same symmetry factor k=5 and hence the same recombination center was used for all three fittings. Only the density of the recombination center was adjusted. Furthermore only one trapping center could be used for all three fittings. This implies, that similar defects are present at least in the middle part of the ingot with varying defect densities only.

With these simulations and measurements it is demonstrated once again, that trapping effects must not be neglected. Particularly, if the working conditions of a solar cell are simulated, which are approximately at an injection of 1×10^{13} to 5×10^{14} cm^{-3}, these effects have to be taken into account.

It should be emphasized ones more, that with the here used simulation tool also µPCD measurements can be simulated and fitted, if the exact injection level is known.

B. Comparison of µPCD and MDP

Another application of the presented rate equation system is the possibility of a detailed comparison of different measurement techniques. The main differences between QSSPC, MDP, or µPCD are the illumination conditions. QSSPC and MDP use long light pulses in order to achieve a steady state condition, whereas µPCD uses a very short (200 ns) intense light pulse.

Figure 5(a) shows simulated injection dependent lifetime curves for different length of the exciting light pulse. If a short light pulse is applied the apparent lifetime is much smaller especially at low injection than for steady state conditions. The reason is, that the trapping levels are not saturated completely with carriers for short pulses. After the light

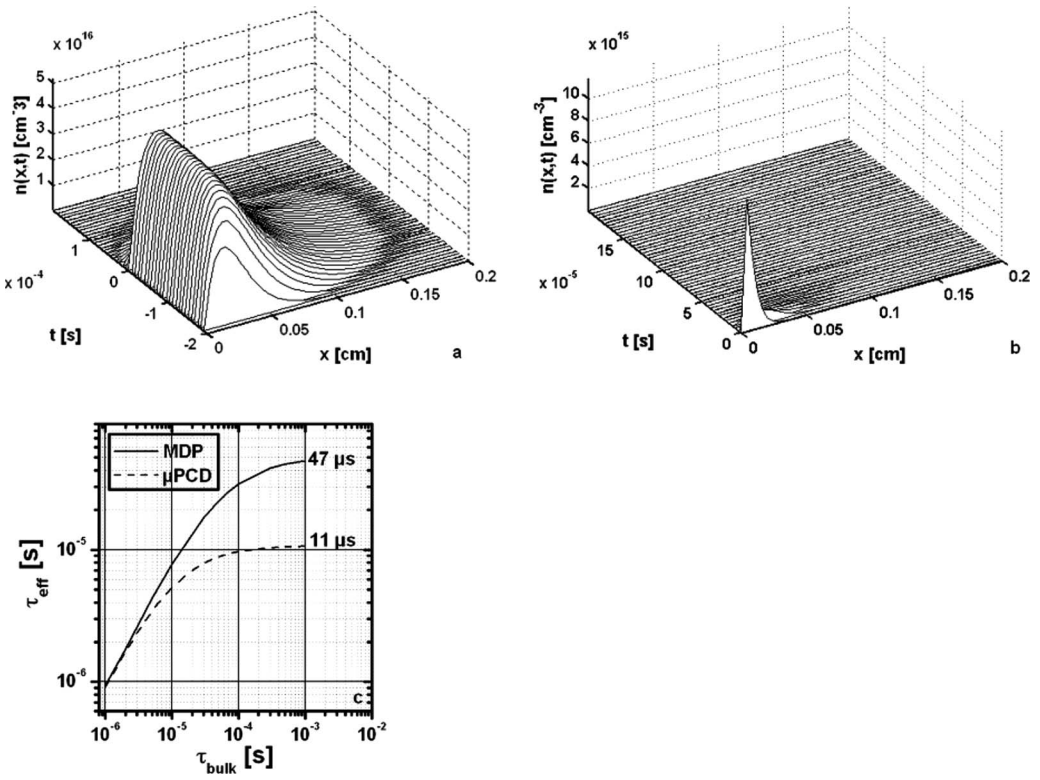

FIG. 6. Carrier profile in a 2 mm thick as-grown ($S=2\times10^5$ cm s^{-1}) sample with $N_{dot}=10^{16}$ cm^{-3} at 300 K for a typical MDP measurement (a) defined by light pulse duration of 200 μs, $\lambda=978$ nm, microwave frequency $\nu=9.4$ GHz and a optical generation rate G_{opt} of 3×10^{21} cm^{-3} s^{-1} and a μPCD. (b) Measurement defined by light pulse duration of 200 ns, $\lambda=904$ nm, $\nu=10.4$ GHz, and a G_{opt} of 5×10^{22} cm^{-3} s^{-1} for both cases FeB was used as the recombination center as defined in Ref. 15; evaluated effective lifetime as a function of bulk lifetime for MDP and μPCD. (c) Ref. 11.

pulse is switched-off, in addition to the recombination, trapping into the not saturated levels occurs. This effect leads to a faster depletion of the bands and hence to a smaller apparent lifetime. Figure 5(b), which shows the time dependent trap occupation for different lengths of the exciting light pulses, underlines this statement. Whereas steady state conditions (200 μs) lead to a decreasing trap occupation after the light is switched-off, for shorter light pulses the trap levels are still filled during the transient. Figure 5(c) displays injection dependent MDP measurements performed with a 3 and 200 μs light pulse. These measurements confirm the simulations because they clearly show a smaller apparent lifetime at low injections for the short (3 μs) light pulse.

C. Measurements on thick samples

As mentioned before, it is vital to simulate the carrier profiles, that develop in a thick sample during the measurement to correctly interpret the lifetime results.

Figure 6 displays the simulation results for the carrier profiles of a MDP measurement using (a) a pulse length of 200 μs and (b) a μPCD measurement performed with a very short light pulse of only 200 ns. It becomes evident, that the MDP conditions, or more generally speaking: steady state conditions, generate carrier profiles, that expand much deeper into the sample. During the comparatively long light pulse of MDP a steady state is reached. That means, a stable diffusion profile of the carriers is developed in the sample. Contrary to that, there is not enough time for diffusion during the very short light pulse of a μPCD measurement. That is why a very surface near carrier profile develops.

As a result, the carrier density decays much faster for nonsteady-state than for steady-state conditions because the surface recombination has a much larger impact. This obviously leads to a smaller apparent lifetime.

To investigate the quantitative effect Fig. 6(c) displays the simulated effective lifetimes for MDP and μPCD conditions for different bulk lifetimes. As anticipated from the carrier profiles, the surface effect strongly influences μPCD measurements but is less pronounced in MDP measurements. This leads to an increasing difference between effective lifetimes determined with MDP and μPCD with increasing bulk lifetime. For very high bulk lifetimes the effective lifetime saturates at about 11 μs for μPCD and 47 μs for MDP. Measurement result confirming these theoretical results are reported elsewhere by our group.[11]

V. CONCLUSIONS

Using both a generalized rate equation system and a partial differential equation system allows the theoretical investigation of the influence of different measurement conditions and trapping effects. The simulation tool presented is proved to be valuable for the calculation of effective lifetimes of thick samples as well as for the investigation of very complex defect models. Based on simulation results this paper shows that the different illumination conditions used in different lifetime determination methods can result in a different behavior of the photogenerated carriers, especially when

trapping occurs or measurements on thick as-grown samples are performed. These theoretical results are furthermore confirmed by experimental experiences obtained by adequate measurements. In order to provide a sound basis for the interpretation of very different experimental results obtained under different experimental conditions and to achieve a better understanding of the carrier dynamics during the measurements, simulations as presented above therefore might be helpful in the future. They might be also increasingly promising in terms of material characterization in order to design the best experimental conditions and strategies to obtain a realistic picture of, e.g., the working conditions of a solar cells. With such experiments and simulations it might become easier to decide whether or not a given material is suitable for solar cell applications.

[1]W. Shockley and W. T. Read, Phys. Rev. **87**, 835 (1952).
[2]J. A. Hornbeck and J. R. Haynes, Phys. Rev. **97**, 311 (1955).
[3]K. R. McIntosh, B. B. Paudyal, and D. H. Macdonald, J. Appl. Phys. **104**, 084503 (2008).
[4]M. J. Brasil and P. Motisuke, J. Appl. Phys. **68**, 3370 (1990).
[5]O. Yoshie and M. Kamihara, Jpn. J. Appl. Phys., Part 1 **22**, 621 (1983).
[6]S. Schmerler, T. Hahn, S. Hahn, J. Niklas, and B. Gründig-Wendrock, J. Mater. Sci.: Mater. Electron. **19**, 328 (2008).
[7]T. Hahn, S. Schmerler, S. Hahn, and J. R. Niklas, J. Mater. Sci.: Mater. Electron. **19**, 79 (2008).
[8]A. C. Hindmarsh, J. Sci. Comput. **1**, 55 (1983).
[9]P. N. Brown and A. C. Hindmarsh, Int. J. Appl. Math Comput. Sci. **31**, 40 (1989).
[10]J. M. Dorkel and P. Leturcq, Solid-State Electron. **24**, 821 (1981).
[11]N. Schueler, K. Dornich, J. R. Niklas, and B. Gruendig-Wendrock, Sol. Energy Mater. Sol. Cells (2010) (to be published).
[12]W. E. Schiesser, *The Numerical Method of Lines* (Academic, San Diego, 1991).
[13]T. Hahn, Thesis, TU Bergakademie, 2009.
[14]S. Rein and S. W. Glunz, Appl. Phys. Lett. **82**, 1054 (2003).
[15]S. Rein and S. W. Glunz, J. Appl. Phys. **98**, 113711 (2005).
[16]N. Schueler, T. Hahn, K. Dornich, and J. R. Niklas, Solid State Phenom. **156-158**, 241 (2010).